MODELING OF RADIAL MICROSTRIP BENDS

A. Weisshaar, S. Luo, M. Thorburn and V.K. Tripathi, Oregon State University, OR
M. Goldfarb, Raytheon Research Laboratories, Lexington, MA
J.L. Lee and E. Reese, Texas Instruments Microwave Laboratory, Dallas, TX

ABSTRACT

Equivalent curved waveguide and lumped circuit models are presented and used to compute the transmission characteristics of radial microstrip bend discontinuities. The calculated results are compared with both transmission and resonance measurements to validate the accuracy of the models. The conductor and radiation losses for the bend discontinuity are included in the model.

I. INTRODUCTION

Even though a considerable amount of work has been reported on the modeling and characterization of right-angled bends, the work reported on curved microstrip bends has been primarily limited to quasi-static computation of excess inductances and capacitances [1,2]. In this paper, the equivalent circuit as well as the planar waveguide models are used to study the microstrip radial bend discontinuities. Resonance and transmission measurement techniques are used to characterize the radial bend discontinuities, and the measured data are compared with the calculated results.

II. THEORETICAL FORMULATION

A lumped equivalent circuit model is derived in terms of the capacitance and the inductance of the circular sector between the two microstrips (Figs. 1(a) and 1(b)). The circular sector is assumed to have the charge and current distribution corresponding to a microstrip ring having the same inner and outer radius. For the ring, the capacitance is computed by utilizing the spectral domain technique in the Fourier-Bessel transform domain with Chebychev polynomials for the basis and test functions [3]. The inductance is obtained by assuming that the current distribution corresponds to the charge distribution for this quasi-TEM approximation. The inductance can then be computed by using the vector potential and the associated energy function.

In order to characterize the discontinuity more accurately and to compute the frequency-dependent transmission characteristics of the radial bend , a curved planar waveguide discontinuity model has also been developed. The microstrip geometry and the waveguide model parameters are shown in Figures 1(a) and 1(c). The model is similar to the one used for microstrip rings (e.g., [4]) with a frequency-dependent effective width and frequency-dependent effective permittivity corresponding to the straight microstrip sections [5], and with the effective mean radius of curvature, R_e, given in Fig. 1(c). This R_e is chosen to ensure a positive effective inner radius for all values of the microstrip inner and outer radius.

The frequency-dependent transmission characteristics of the radial microstrip bend are derived by utilizing a second-order perturbation analysis [6] of the equivalent modified curved waveguide model together with a mode-matching technique [7-9] which includes the higher-order modes. This mode-matching technique requires a complete set of transversal field solutions with orthogonal properties in all three regions. A complete, orthogonal set of solutions for the fields in the two straight regions I and II which consists of an infinite series with a TEM mode and TE_{no} modes (n=1, 2, ...) is given in [8,9]. For region III we introduce the curved orthogonal coordinate system (Fig. 1(c)) characterized by $u_1=x$, $u_2=y$, and $u_3=s=R_e\phi$ with corresponding metric coefficients $h_1=h_2=1$ and $h_3=1+y/R_e$ [4,6]. Then the field solutions for the transversal field component E_x in region III are given by

$$E_n = f_n(y)\, e^{-j\beta_n s} \qquad (1)$$

These form a complete set of eigenfunctions which are orthogonal with respect to the weighting function $(1 + y/R_e)^{-1}$ [6], i.e.,

$$\int_{-w_e/2}^{w_e/2} E_m E_n (1+y/R_e)^{-1} = 0 \qquad \text{for } m \neq n. \qquad (2)$$

CH2848-0/90/0000-1051$01.00 © 1990 IEEE

The total transverse electric field component E_x is then given as an infinite series in the eigenfunctions E_n with unknown coefficients c_n:

$$E_x = \sum_{n=0}^{\infty} c_n E_n \tag{3}$$

A perturbation solution for E_n can be found by expanding f_n and β_n^2 along s in a power series in the effective radius of curvature R_e of the curved waveguide as shown in [6] for a curved waveguide with electric walls:

$$f_n = \Phi_{on} + \frac{\Phi_{1n}}{R_e} + \frac{\Phi_{2n}}{R_e^2} + \ldots \tag{4a}$$

$$\beta_n^2 = \beta_{on}^2 \left(1 + \frac{B_{1n}}{R_e} + \frac{B_{2n}}{R_e^2} + \ldots\right) \tag{4b}$$

Here, Φ_{on} and β_{on} are the solutions for a straight waveguide (R and $R_e \to \infty$). For a second-order perturbation solution which represents an extension of the first-order solution reported in [4], the expansion functions Φ_{1n} and Φ_{2n} as well as the expansion constants B_{1n} and B_{2n} are given in [6]. A form of field solutions suitable for the mode-matching method is constructed by alternately placing a magnetic wall at the junctions of the straight and curved waveguides, i.e., at s=0 and $s=R_e\alpha$ (Fig. 1(c)). The scattering parameters for the TEM mode are then computed in terms of the amplitudes of the transmitted and reflected waves after applying the mode-matching technique as in [7-9]. The difference between the real electrical length of the curved microstrip region and model electrical length is used to correct the phase of the scattering parameters.

The electric and magnetic fields inside the curved cavity region at the magnetic walls are also computed in terms of the magnitude of the incident wave. These can be used to estimate conductor loss, radiation loss, and coupling between bends. The conductor loss is calculated in terms of the tangential magnetic field at the conductor surface in the curved region and the radiation loss is calculated in terms of the aperture electric fields at the magnetic walls as shown in [11] for other microstrip discontinuities.

III. THEORETICAL RESULTS

The scattering parameters of typical radial bends on Alumina and GaAs substrate for various line widths ranging from low (e.g., 20Ω) to high (e.g., 80Ω) impedance lines have been computed as a function of frequency. In addition, the equivalent lumped parameters for various geometries have been computed by using the quasi-static technique. Figure 2 shows the reflection coefficient corresponding to two cases of 50° radial bend discontinuities. The agreement is seen to be quite good at low frequencies and for thin substrate circuits where the quasi-static approximation is valid.

The waveguide model calculations exhibit good convergence behavior with increasing number of higher-order modes considered in the series expansions for the field solutions, and for most cases five higher-order modes lead to a converged, accurate solution. For example, Figure 3 shows the reflection coefficient for a nominal 30Ω, 90° microstrip bend with R=2w on a 0.635mm Alumina substrate. Results for the corresponding right-angle and chamfered right-angle bends based on empirical CAD expressions as given in [10] are also included in the figure for comparison. Note that the first higher-order mode (TE_{10} mode) propagates above approximately 20GHz as indicated in the figure. Whereas empirical CAD expressions or other equivalent circuits do not directly reflect the influence of propagating higher-order modes on the transmission characteristics, these higher-order modes are automatically included in the waveguide models as shown in Fig. 3. Figure 4 shows the normalized radiation loss for the cases of nominal 50W lines on 25 mil Alumina and 4 mil GaAs substrate. For both cases, the radius of curvature is taken to be twice the strip width, and as expected, the microstrip bend on the thicker Alumina substrate has higher radiation loss.

IV. EXPERIMENTAL RESULTS

Figure 5 shows the measured data for the reflection coefficient for eight 90° bends having R=w=70μm on a 100μm GaAs substrate cascaded by straight sections of microstrips (see inset) together with the calculated results based on the waveguide model. The agreement is found to be excellent. Similar agreement is found for the measured phase response, S_{21}, and for structures with bends having larger radius, e.g. R=2w.

Figure 6 shows the results for S_{21} of a microstrip on a 5 mil Alumina substrate with an open stub. As shown in the inset, the stub consists of a straight microstrip terminated in a radial section and an open microstrip end section. Measurements were also made with a straight microstrip open ended stub to extract any errors introduced due to the microstrip T and the microstrip open end models. Again, the measured resonance data are in excellent agreement with the calculated values based on the waveguide model. The TI model in this figure is based on an empirical correction for phase reduction due to bending of the microstrips. Other resonance measurements have been made for wider and narrower microstrips with different values of microstrip radius for the curved bend regions, and agreement between the measured data and the calculated values has been found to be excellent.

REFERENCES

[1] R.K. Hoffman, Handbook of Microwave Integrated Circuits, Artech House, 1987.

[2] P. Anders and F. Arndt, "Beliebig abgeknickte Microstrip-Leitungen mit bogenförmigem Übergang," *Arch. Elek. Übertragung.*, vol. 33, pp. 93-99, March 1979.

[3] A. Sharma and B. Bhat, "Spectral domain analysis of microstrip ring resonators," *Arch. Elek. Übertragung.*, vol. 33, pp. 130-132, 1979.

[4] V.K. Tripathi and I. Wolff, "Perturbation analysis and design equations for open- and closed-ring microstrip resonators," *IEEE Trans. Microwave Theory Tech.*, vol. MTT-32, pp. 405-410, Apr. 1984.

[5] G. Kompa and R. Mehran, "Planar waveguide model for microstrip discontinuities and T-junctions," *Electron. Lett.*, vol. 11, pp. 459-460, Sept. 1975.

[6] L. Lewin et al., Electromagnetic Waves and Curved Structures, New York: IEEE Press, 1977.

[7] E. Kühn, "A mode-matching method for solving field problems in waveguide and resonator circuits," *Arch. Elek. Übertragung.*, vol. 27, pp. 459-460, Sept. 1975.

[8] W. Menzel and I. Wolff, "A method for calculating the frequency dependent properties of microstrip discontinuities," *IEEE Trans. Microwave Theory Tech.*, vol. MTT-25, pp. 107-122, Feb. 1977.

[9] I. Wolff, "The waveguide model for the analysis of microstrip discontinuities," in Numerical Techniques for Microwave and Milimeter Wave passive Structures, Ed. T. Itoh, Wiley, 1989.

[10] M. Kirschning and R.H. Jansen, "Accurate wide-range design equations for the frequency dependent characteristic of parallel coupled microstrip lines," *IEEE Trans. Microwave Theory Tech.*, vol. MTT-32, pp. 83-90, Jan. 1984.

[11 A. Sabban and K.C. Gupta, "Multiport network model for evaluating radiation loss and spurious coupling between discontinuities in microstrip circuits," *IEEE MTT-S Intl. Microwave Symp. Dig.*, pp. 707-710, Long Beach, June 1989.

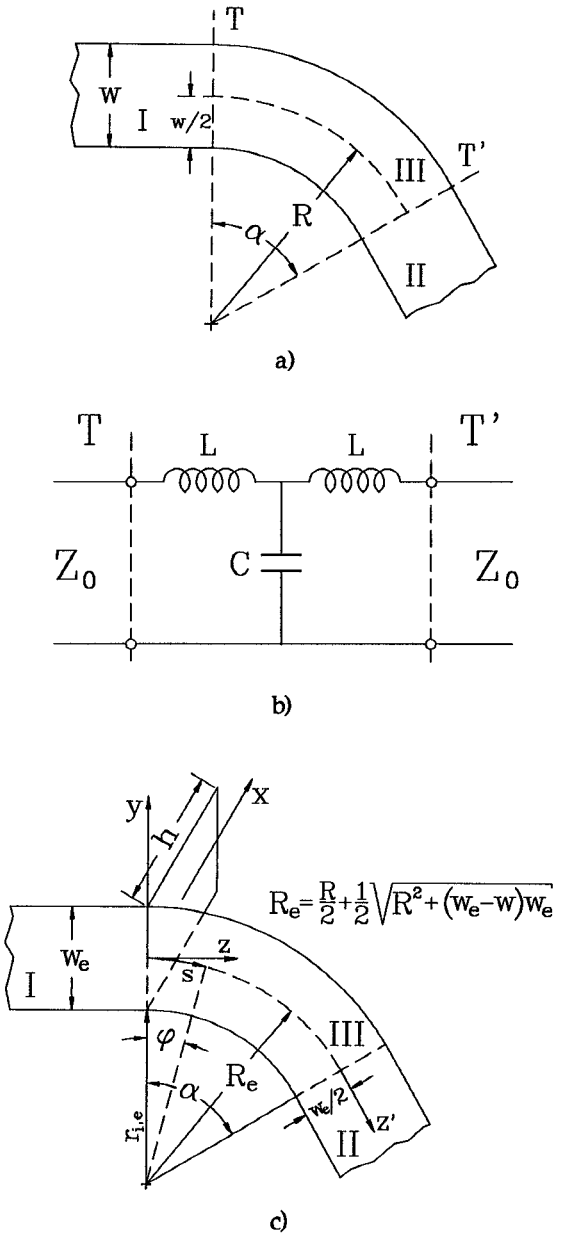

Fig. 1: (a) Microstrip bend, (b) equivalent lumped model, (c) waveguide model

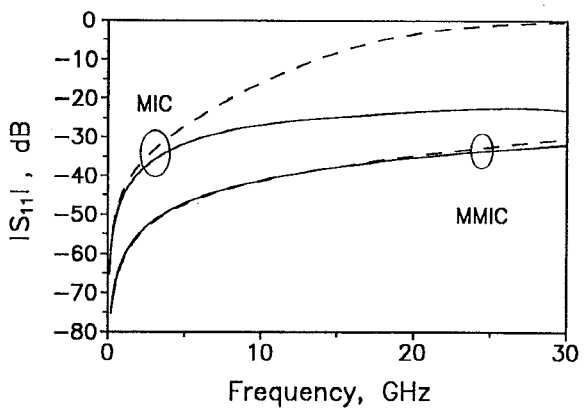

Fig. 2: S_{11} for 50Ω, 90° bends with R=2w on MIC - 25mil Alumina and MMIC - 4mil GaAs substrate (——— waveguide model, ------ quasi-static model).

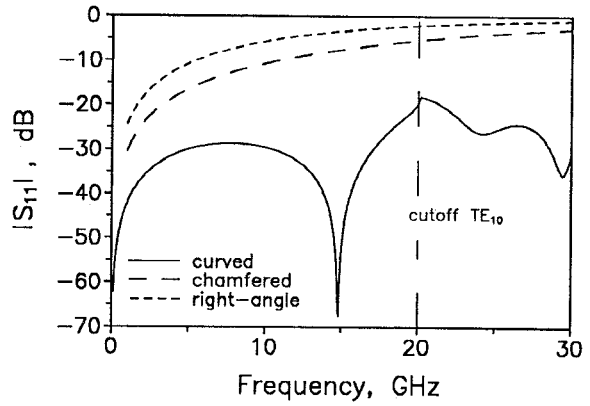

Fig. 3: S_{11} for a 30Ω, 90° bend on a 25 mil Alumina substrate (R=2w).

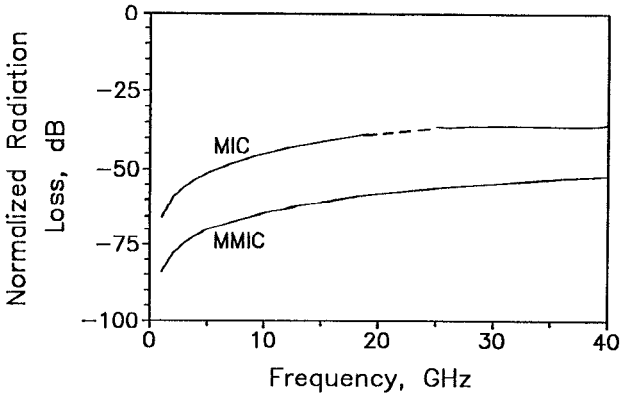

Fig. 4: Normalized radiation loss for 50Ω bends with R=2w on MIC - 25 mil Alumina and MMIC - 4 mil GaAs substrate.

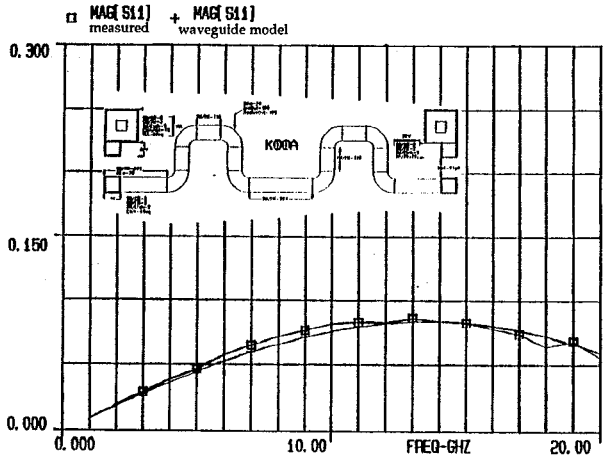

Fig. 5: Measured and calculated S_{11} for the circuit shown in the inset (w=70μm, h=100μm, ε_r=12.88).

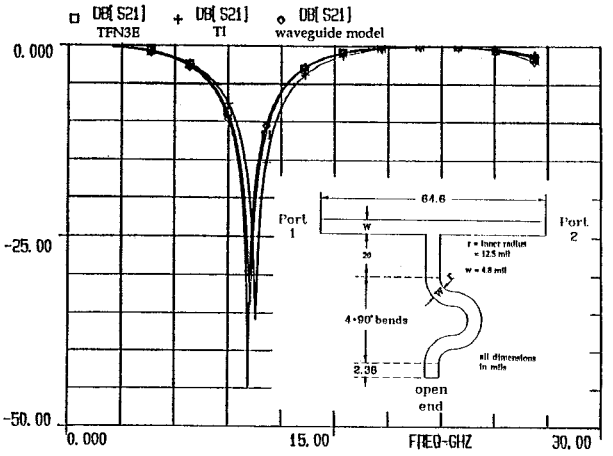

Fig. 6: S_{21} for a microstrip T with an open stub having curved bends (h=5mils, ε_r=9.9).